Available online at www.sciencedirect.com
SCIENCE DIRECT
Journal of Power Sources 158 (2006) 94–102
JOURNAL OF POWER SOURCES
www.elsevier.com/locate/jpowsour

Experimental determination of effective surface area and conductivities in the porous anode of molten carbonate fuel cell

Masahiro Yoshikawa [a,*], Andreas Bodén [b], Mari Sparr [b], Göran Lindbergh [b]

[a] *Central Research Institute of Electric Power Industry, Sector Advanced Power Engineering, Energy Engineering Research Laboratory, Yokosuka-shi, Kanagawa 240-0196, Japan*
[b] *Department of Chemical Engineering and Technology, Applied Electrochemistry, Royal Institute of Technology (KTH), SE-100 44 Stockholm, Sweden*

Received 9 July 2005; received in revised form 15 September 2005; accepted 23 September 2005
Available online 9 November 2005

Abstract

Stationary polarization curves and electrochemical impedance spectroscopy of a porous nickel anode in a molten carbonate fuel cell were obtained in order to determine the active surface area and conductivities with varying degree of electrolyte filling for two anode feed-gas compositions, one simulating operation with steam reformed natural gas and the other one gasified coal. The active surface area for coal gas is reduced by around 70–80% compared to the standard gas composition in the case of Li/Na carbonate. Moreover, an optimal degree of electrolyte filling was shifted toward higher filling degree in the case of operation with coal gas.

In order to evaluate the experimental data a one-dimensional model was used. The reaction rate at the matrix/electrode interface is about five times higher than the average reaction rate in the whole electrode in case of 10% electrolyte filling. This result suggests that the lower limit of the filling degree of the anode should be around 15% in order to avoid non-uniform distribution of the reaction in the electrode. Therefore, in the case of applying Li/Na carbonate in the MCFC, an electrolyte distribution model taking into account the wetting properties of the electrode is required in order to set an optimal electrolyte filling degree in the electrode.

Keywords: Molten carbonate fuel cell; Porous anode; Electrochemical impedance spectroscopy; Effective conductivity

1. Introduction

The molten carbonate fuel cell (MCFC) is considered to be one of the most promising power generation systems. The MCFC is in general operated using natural gas as fuel, although high concentrations of carbon monoxide and carbon dioxide can also be a part of the feed. This makes it very suitable for use with lower concentrations of hydrogen as found in biogas, coal gasification gas, waste gas or gasified biomass. Especially operation with biogas or waste gas reduces the use of fossil fuel and greenhouse gas emissions. However, it has been reported that the degradation rate of cell voltage is higher in the case of 'CO-rich fuel conditions' than in the case of 'H_2-rich fuel conditions', and consequently, the cell performance becomes unstable [1]. Moreover, oxidation and agglomeration of nickel particles at the electrolyte side of the anode has also been observed. This high degradation rate under the 'CO-rich fuel conditions' depends on the growth of the cathode reaction resistance, the anode reaction resistance and the internal resistance [1].

Every electrode has its optimal electrolyte filling degree, i.e. the best performance for given conditions, but due to changes such as sintering of particles, this optimum might change during long-term operation. Therefore, when designing and manufacturing porous electrodes for MCFC the goal might be to have as good performance as possible for as large a filling degree interval as possible.

Operation with low concentration of hydrogen increases the losses at the anode [2], a contribution to the increased loss through the change of the wetting angle due to the change of gas composition [3]. Moreover, this affects the electrolyte distribution which might change the active surface area and effective electrolyte conductivity.

* Corresponding author. Tel.: +81 46 856 2121; fax: +81 46 856 3346.
E-mail address: yoshika@criepi.denken.or.jp (M. Yoshikawa).

0378-7753/$ – see front matter © 2005 Elsevier B.V. All rights reserved.
doi:10.1016/j.jpowsour.2005.09.038

Nomenclature

C_d	total geometric double layer capacitance ($F\,m^{-2}$)
c_d	intrinsic double layer capacitance ($F\,m^{-2}$)
i	total current density ($A\,m^{-2}$)
i_2	electrolyte phase current density ($A\,m^{-2}$)
j	imaginary number
j_2	dimensionless current density in electrolyte phase
$L_{electrode}$	thickness of electrode (m)
$L_{mat\text{-}act}$	the vertical distance between electrode/matrix interface and reference electrode (m)
m	constant in Archie's law
R_a	local reaction resistance ($\Omega\,m^2$)
R_{an}	anode reaction resistance ($\Omega\,m^2$)
$R_{c.c.}$	resistance of current collector ($\Omega\,m^2$)
$R_{contact}$	contact resistance between the electrode particles ($\Omega\,m^2$)
R_{ct}	total charge-transfer resistance ($\Omega\,m^2$)
R_Ω	total solution resistance ($\Omega\,m^2$)
R_{mat}	total matrix resistance ($\Omega\,m^2$)
$R_{particle}$	resistance of the electrode particles ($\Omega\,m^2$)
R_{pore}	resistance of pore electrolyte in the electrode ($\Omega\,m^2$)
R_{wire}	resistance of lead wire ($\Omega\,m^2$)
S_{act}	active surface area ($m^2\,m^{-3}$)
S_{spec}	specific surface area per unit volume ($m^2\,m^{-3}$)
W_R	resistance in Warburg impedance ($\Omega\,m^2$)
W_S	Warburg impedance ($\Omega\,m^2$)
x	electrode depth (m)
y	dimensionless electrode depth
Z	total impedance ($\Omega\,m^2$)

Greek symbols

ε	porosity
η_a	anode polarization (V)
κ	free electrolyte conductivity, $230\,S\,m^{-1}$ at 923 K
κ_{eff}	effective conductivity of pore electrolyte in the electrode ($S\,m^{-1}$)
θ	electrolyte degree of filling
σ_{eff}	effective conductivity of electrode ($S\,m^{-1}$)
τ	time constant
υ	uniformity factor of reaction rate
ω	frequency (Hz)
ψ	fitting parameter

In this study, stationary polarization curves and electrochemical impedance spectroscopy data were obtained in order to determine the active surface area and effective electrolyte conductivities in porous nickel anodes with varying electrolyte filling degree using two different gas compositions. An impedance model was used to evaluate the experimental data. This study also provides basic data for designing the morphology of the electrodes and combinations of electrodes in order to prolong the cell life for different gas compositions. These results can be used in cell and stack models for system simulations.

2. Experimental

Characterization of the electrodes has been performed by means of two electrochemical measurement techniques: electrochemical impedance spectroscopy (EIS) and DC polarization curve measurements. The former is a transient technique, enabling elucidation of the mechanism of fast electron-transfer reactions and diffusion resistance in molten carbonate. The latter is a steady-state technique, used to measure the sum of reaction resistances in order to verify the impedance data. The laboratory fuel cell equipment is depicted schematically in Fig. 1. In this conventional set-up, the reference electrodes are made of gold wires placed in separate chambers filled with electrolyte. These chambers are connected to the electrolyte matrix through a hole filled with electrolyte and gold wires. The electronic current flow is established through the nickel current collectors.

A symmetric laboratory cell with two identical electrodes was used in order to investigate the effect of electrolyte filling degree in the electrode. Both electrodes were fed with the same gas.

Experimental data were obtained from a 3 cm^2 laboratory cell unit. The specifications of the materials are listed in Table 1. All the experiments were carried out using two different gas compositions as shown in Table 2. The anode gas was humidified at 60 °C. In order to reduce the effect of conversion and mass-transfer limitations in the gaseous phase, the gas flow rate was kept high and the gas utilization was calculated to be less than

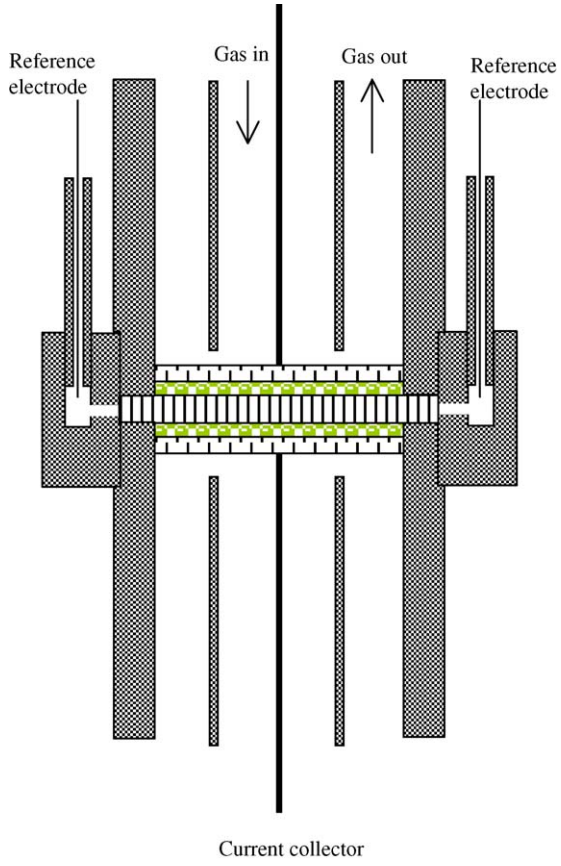

Fig. 1. Schematic drawing of laboratory cell unit used for experiment.

Table 1
Specification of the different anodes used in experiments

	Anode A	Anode B	Anode C
Size (cm^2)	3	3	3
Thickness (cm)	0.078	0.071	0.066
Material	Ni–Al alloy	Ni–Cr alloy	Ni–Al alloy
Porosity (%)	52	58	45
Counter electrode	Anode A	Anode B	Anode C
Carbonate	Li/Na	Li/K, Li/Na	Li/K

Table 2
Gas compositions

	H_2	CO	CO_2	N_2	H_2O
Standard gas	64	0	16	0	20
Coal gas	12	24	40	4	20

1%. Two different electrolytes were investigated, a 62/38 mole% Li/K carbonate melt or a 52/48 mole% Li/Na carbonate melt. DC polarization curve measurements and EIS measurements were obtained at electrolyte filling degrees between 0 and 100%, respectively. The filling degree is defined as the part of the void volume of the electrode filled with electrolyte. The void volume was calculated from the initial electrode volume, density and weight. In this study, carbonate grains were added to the electrode in order to increase the electrolyte filling degree. The total initial amount of electrolyte for the whole cell was chosen so that the whole matrix would be completely filled.

The EIS measurements were carried out using Solartron 1250 FRA and a Solartron 1286 or 1287 potentiostat. The frequency spectra were recorded at open circuit potential in the frequency range 2 kHz–10 mHz and with an amplitude of 10 mV.

The current interrupt method was used for evaluating the ohmic potential drop in DC polarization measurements. In these measurements, the overvoltage was recorded 20 μs after interruption of the current.

3. Results and discussion

3.1. Anode reaction resistance obtained from DC polarization measurements

Fig. 2 shows the *iR*-corrected polarization curves obtained from DC polarization measurement at different electrolyte filling degrees for Li/Na carbonate at the standard gas composition for anode B. A linear relationship between the current density and the anode polarization, η_a, was found in the experimental polarization curve at low overvoltage. Regarding the linear range, a voltage drop caused by the anode polarization can be described approximately as an anode reaction resistance given by:

$$\eta_a \cong R_{an} \cdot i \quad (1)$$

where R_{an} denotes the anode reaction resistance due to the polarization in the anode and i is the total current density. The anode reaction resistance was determined from the slope of the anode

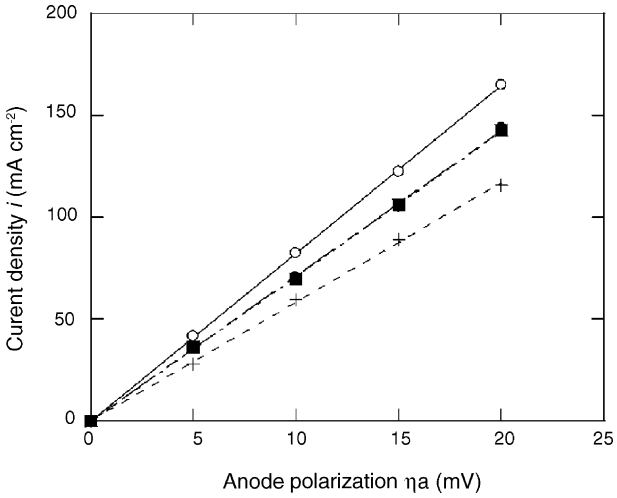

Fig. 2. Polarization curves at different electrolyte filling degrees for anode B, (◯) 9%, (●) 24%, (■) 49%, (+) 80%.

polarization curves. In EIS measurements, this corresponds to the difference between the low and high frequency real part intercepts.

In Fig. 3, the relationship between the anode reaction resistance obtained from DC polarization measurements and that obtained from EIS measurements is shown for Anode B using Li/Na carbonate. As can be seen the same anode reaction resistances were obtained from both techniques.

In Fig. 4(a–c) the relationship between the electrolyte filling degree and anode reaction resistance is shown for Li/K carbonate and Li/Na carbonate for the two gas compositions. The reaction resistances were calculated from polarization curves. These figures also demonstrate the optimal degree of electrolyte filling for the different electrodes.

Comparing the reaction resistance of anode B and anode C, Fig. 4(c), it may be observed that the reaction resistance of anode C is more strongly influenced by electrolyte filling degree than anode B. The pore size distributions of these electrodes were

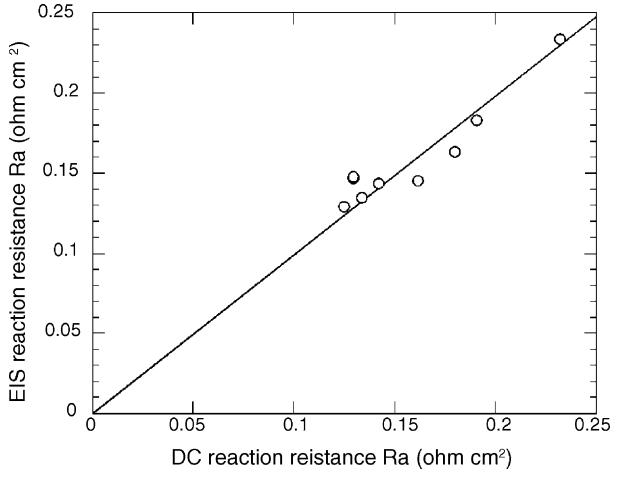

Fig. 3. Relationship between the reaction resistances obtained from DC polarization measurements and the reaction resistances from EIS measurements for anode B using Li/Na carbonate and standard gas. (—) Equal value line and (◯) measured values.

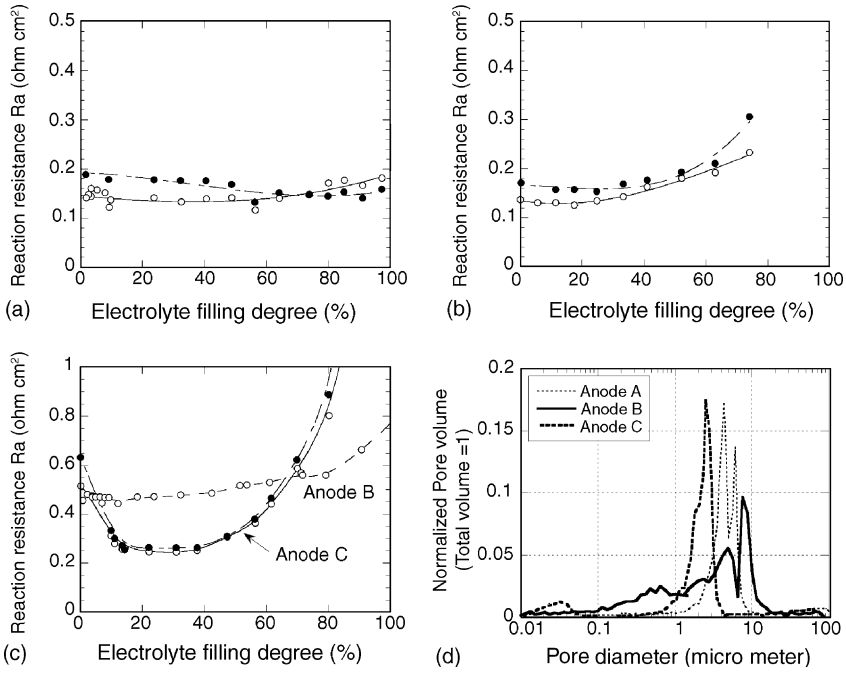

Fig. 4. The anode reaction resistance dependence as a function of the electrolyte filling degree for (a) anode A with Li/Na carbonate; (b) anode B with Li/Na carbonate and (c) anodes B and C with Li/K carbonate, for two different gas compositions (◯) standard gas and (●) coal gas; (d) the pore size distribution for the three different anodes.

obtained by Hg porosimetry, Fig. 4(d). The macro-pores and micro-pores are clearly seen in anode B, meanwhile only one peak at around three micrometers was observed in anode C. Thus, it is clear that the reaction resistance of an anode is influenced by the pore size distribution and that the bimodal porous structure seems to be advantageous for the anode in order to get a stable performance for varying degrees of filling in the electrode.

Regarding the Li/Na carbonate and the Li/K carbonate, Fig. 4(a and c) the behaviour is different. In the anodes A and B with Li/Na carbonate, the maximum performance is obtained at a fill of about 10–50% for anode A and 5–20% for anode B in case of operation with standard gas. On the other hand, in case of operation with coal gas, an optimal degree of electrolyte filling was shifted toward higher filling degree. Regarding anode C in Li/K carbonate, Fig. 4(c), there was no remarkable change of the optimal electrolyte filling degree between the standard gas and coal gas, but the reaction resistance increased slightly when using coal gas.

According to data of wetting angles [1], the calculated contact angles for the anode at standard gas conditions is 50° and for coal gas 61° in Li/Na carbonate, and 31° and 40° in the Li/K carbonate case, assuming a polarization of 0.02 V at 923 K with the gases being completely reformed through the water–gas shift reaction. Therefore, the anode in Li/K carbonate is better wetted than in Li/Na carbonate. A possible cause for the unchanged optimal electrolyte filling degree in the case of Li/K carbonate might be the slight change of active surface area caused by the good wetting properties of the anode for both gases. On the other hand, the anode in Li/Na carbonate is not well wetted due to larger contact angles. The optimal filling degree was shifted toward higher filling degree in the case of coal gas operation because of decreased amount of active surface area in the anode.

As mentioned above in the case of applying Li/Na carbonate to the MCFC, an electrolyte distribution model taking the wetting properties of the electrode into account is required in order to set as optimal electrolyte filling degree in the electrode.

3.2. Electrochemical impedance spectroscopy of the anode

The Nyquist diagram of anode A, shown in Fig. 5, clearly shows the existence of two loops. Regarding the high-frequency arc (2 kHz–20 Hz), the size of the arc increases with decreasing temperature as shown in Fig. 5(a). On the other hand, regarding the low-frequency arc (20 Hz–10 mHz), the size of the arc does not change with temperature. Fig. 5(b) shows the EIS response of the anode for different gas flows. The size of the high-frequency arc is independent of the flow rate. Regarding the low-frequency arc (20 Hz–10 mHz), the size decreased with increasing flow rate.

As noted above, the size of the high-frequency arc corresponds to the polarization by the charge-transfer process in the anode and the size of the low-frequency arc corresponds to the polarization by mass transfer in the anode [4].

In Fig. 6, the EIS response for anode A is shown at different electrolyte filling degrees for the two gas compositions. Regarding the high-frequency arc, the size of the arc does not change or decreases slightly with increasing the electrolyte filling degree. This is valid for both gas compositions. In addition, the ohmic resistance, at the high-frequency limit, decreases with increasing the degree of electrolyte filling for both gas conditions.

The EIS data show a typical mixture of charge-transfer and mass-transfer control. In order to estimate the size of these arcs

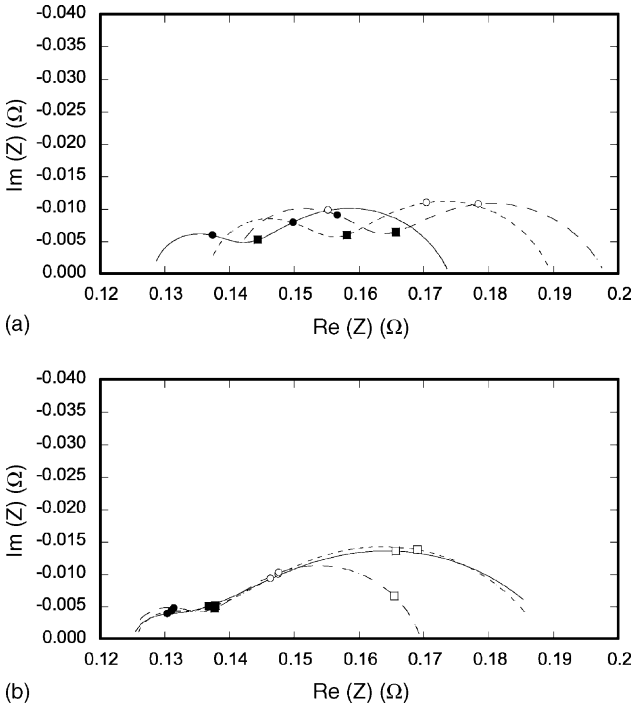

Fig. 5. Electrochemical impedance spectroscopy responses of anode A at open circuit voltage at standard gas conditions for different temperatures at 125 ml min^{-1}. (a) (—) 923 K, (- - -) 886 K, (– –) 865 K, and for different flow rates at 923 K. (b) (—) 25 ml min^{-1}, (- - -) 50 ml min^{-1}, (– –) 125 ml min^{-1}. Some frequencies have been marked: (●) 200 Hz, (■) 20 Hz, (◯) 2 Hz and (□) 0.2 Hz.

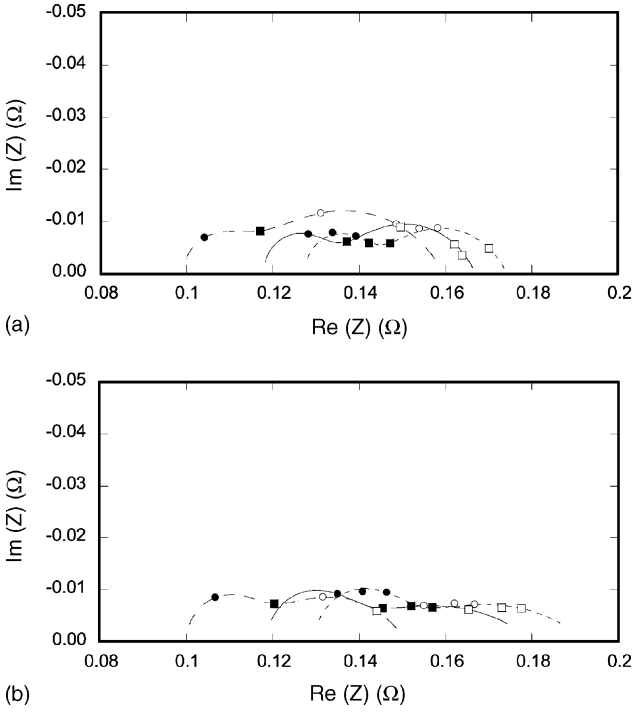

Fig. 6. Electrochemical impedance spectroscopy responses of anode A at different degrees of electrolyte filling, (- - -) 9%, (—) 41%, (– –) 80%, for the two gas composition (a) standard gas and (b) coal gas.

quantitatively, a Randles–Ershler equivalent circuit was applied [5]. This equivalent circuit can be used to evaluate plane dense electrodes but it cannot accurately represent the actual distribution of the double layer capacitance and reaction distribution inside the electrode [6–7]. However, it will be shown later that the reaction rate is quite uniform except for a low degree of filling. The impedance can therefore approximately be given by:

$$Z = R_\Omega + \frac{1}{j\omega C_d + (1/R_{ct} + W_S)} \tag{2}$$

where

$$W_S = W_R \times \frac{\tanh[(j\omega\tau)^\psi]}{(j\omega\tau)^\psi} \tag{3}$$

R_{ct} is the total charge-transfer resistance, C_d the total double layer capacitance, R_Ω the total ohmic resistance, τ the time constant, ψ the constant and W_R is the resistance in Warburg impedance (W_S). These parameters (R_Ω, C_d, R_{ct}, W_R, τ, ψ) were determined by non-linear parameter fitting over the whole frequency range at each measured electrolyte filling degree.

3.3. High-frequency arc

The active surface area, S_{act}, is the total electrode area wetted by electrolyte. The active surface area can be calculated using the intrinsic double layer capacitance, c_d. The intrinsic double layer capacitance is assumed independent of the gas composition and is given in literature [8–9]. The active surface area is estimated from the total double layer capacitance, C_d, using the following relationship:

$$S_{act} = \frac{C_d}{c_d \cdot L_{electrode}} \tag{4}$$

It is clear that the calculated active surface area, Fig. 7, increases with addition of carbonate at both gas compositions. Furthermore, the active surface area for coal gas is lower than for standard gas for both anodes. Regarding an electrolyte filling degree of 10–50% in anode A, it was found that the active surface area for the coal gas is reduced by 70–80% compared to the standard gas composition.

The contact angle for standard gas is calculated to 50°; it is 61° for coal gas as already mentioned [1]. Fig. 8 illustrates how a larger contact angle gives a smaller active surface area at a given degree of electrolyte filling. For a small contact angle, the meniscus wets more of the pore wall with electrolyte than for a larger angle, i.e. the active surface area of electrode changes with the wetting angle. The total active surface can probably not be utilized by the faradic reaction due to too long diffusion length. A change of gas composition will have two major effects on the reaction resistance. It will change the exchange current density and the wetting angle. The wetting angle changes the active surface area and will therefor probably change the available active surface area for the faradic reaction.

It becomes clear that in the case of coal gas operation the optimal filling degree was shifted toward higher values due to

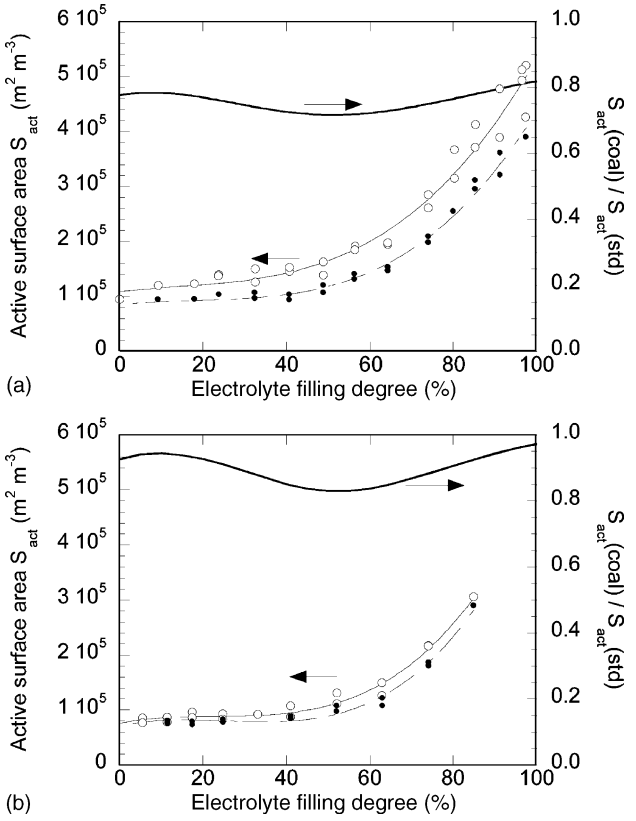

Fig. 7. The active surface area dependence on the electrolyte filling degree of (a) anode A and (b) anode B at 923 K for (◯) standard gas and (●) coal gas.

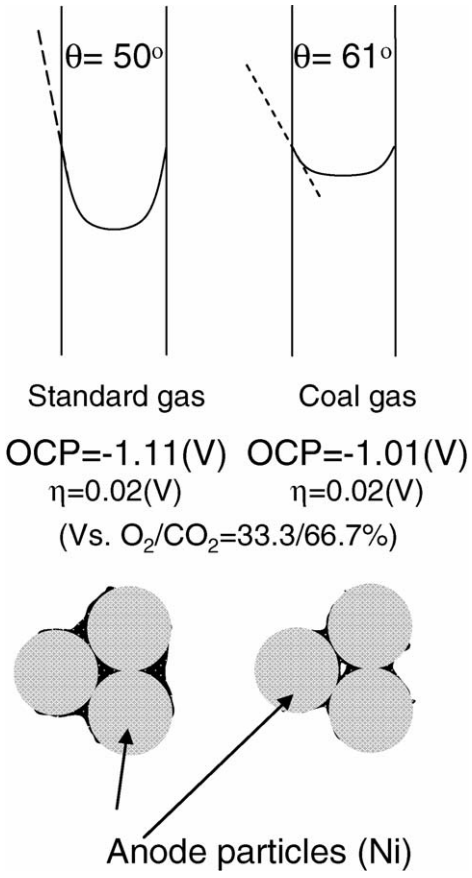

Fig. 8. Illustration of different wetting angles and how these influence the electrolyte in a porous electrode for standard gas and coal gas, respectively.

the decrease of active surface area of the anode. In other words, a higher electrolyte filling degree will be needed as initial criterion in order to obtain as much active surface area as for the standard gas composition when using Li/Na carbonate.

In the case of operation with coal gas using anode A, the increased polarization losses for the coal gas is not only an effect of gas composition but also due to 70–80% reduction of the active surface area compared to the standard gas case.

3.4. Ohmic resistance at the high-frequency limit

The effective conductivity of the electrode, including contact resistance between the particles, and the conductivity of electrolyte inside the pores of the electrode are two important factors in order to understand the reaction rate distribution in a porous electrode. In this study, the EIS data was also used to measure the effective conductivities of the pore electrolyte and the electrode matrix.

The charge transport in a porous electrode is assumed to occur in three steps. The electron-transfer reaction (number 2 in Fig. 9(a)) transfers the current from ionic conduction (number 3 in Fig. 9(a)) in the electrolyte to electronic conduction (number 1 in Fig. 9(a)) in the solid particles. The solid particles make electronic contact with the current collector, which is the perforated plate on top of the electrode.

The ohmic resistance at the high-frequency limit in the impedance measurements must be taken into account in these resistances, as shown in Fig. 9(b).

$$R_{\Omega(\omega\to\infty)} = (R_{\mathrm{mat}} + R_{\mathrm{c.c.}} + R_{\mathrm{wire}}) + \frac{(R_{\mathrm{contact}} + R_{\mathrm{particle}}) \times R_{\mathrm{pore}}}{(R_{\mathrm{contact}} + R_{\mathrm{particle}}) + R_{\mathrm{pore}}} \quad (5)$$

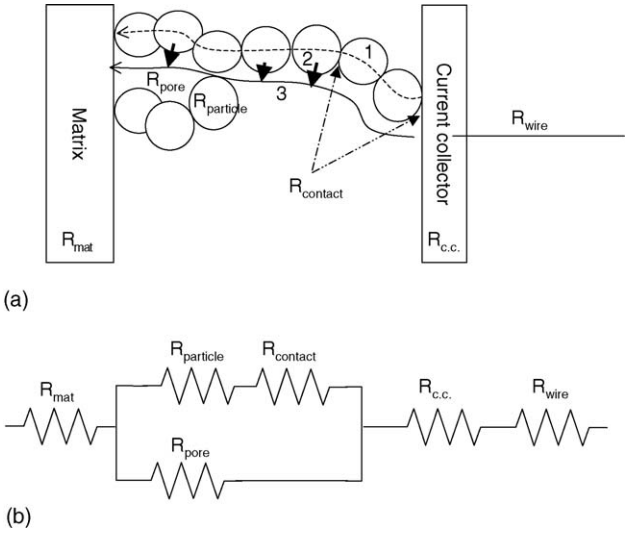

Fig. 9. (a) Current path in a porous electrode, 1 (- - -) electric conductance; 2 (↓) electrochemical reaction, 3 (—) ionic conductance and (b) equivalent circuit at the high-frequency limit in impedance measurement.

Archie's law [10] gives the resistance of pore electrolyte in the matrix:

$$R_{\text{mat}} = \frac{(\varepsilon_{\text{mat}}\theta_{\text{mat}})^{-1.5}}{\kappa} \times L_{\text{mat-act}} \quad (6)$$

where ε_{mat} is the porosity of the matrix, the electrolyte filling degree of the matrix, θ_{mat} is always assured to be one in this study and set by the initial amount of electrolyte and κ denotes the conductivity of the free electrolyte.

In this study, the vertical distance between the electrode/matrix interface and the reference electrode, $L_{\text{mat-act}}$, was treated as a fitting parameter because the EIS were half cell measurements. This distance may vary between different experiments but is constant for each experiment. The reason for this is that the reference electrode was placed in a separate chamber filled with electrolyte and connected at the midsection to the side of the electrolyte matrix as depicted schematically in Fig. 1. As a result of these analyses, the vertical distance between the electrode/matrix interface and the reference electrode were determined to 0.045 cm for anode A and 0.041 cm for anode B.

Archie's law can also be applied to the resistance of pore electrolyte inside the electrode:

$$R_{\text{pore}} = \frac{(\varepsilon_{\text{electrode}}\theta_{\text{electrode}})^{m}}{\kappa} \times L_{\text{electrode}} \quad (7)$$

where $\varepsilon_{\text{electrode}}$ is the porosity of the electrode, $\theta_{\text{electrode}}$ denotes the electrolyte filling degree of the electrode and κ is the conductivity of the free electrolyte.

In this study, the effective conductivity of the electrode is derived from the sum of the resistance of the electrode particles and the contact resistance between the particles.

$$R_{\text{particle}} + R_{\text{contact}} = \frac{L_{\text{electrode}}}{\sigma_{\text{eff}}} \quad (8)$$

The parameters ($L_{\text{mat-act}}$, m, σ_{eff}, κ_{eff}) were determined by non-linear parameter fitting for the whole electrolyte filling degree interval, where only κ_{eff} is assumed to depend on the electrolyte filling degree, as can be seen in Eq. (7).

Fig. 10 shows the ohmic resistance at the high-frequency limit as function of the degree of electrolyte filling. The circle and the square indicate the experimental data, and the solid line shows the fitting result obtained from Eq. (4).

The effective conductivity of the anodes A and B in the solid phase, σ_{eff}, has been determined to 48 and 106 S m^{-1}, respectively, and the effective conductivity of the pore electrolyte in the anode has been determined as a function of the filling degree for Li/Na carbonate:

$$\kappa_{\text{eff}} = \kappa \times (\varepsilon\theta)^{1.68} \quad \text{for anode A} \quad (9)$$

$$\kappa_{\text{eff}} = \kappa \times (\varepsilon\theta)^{1.65} \quad \text{for anode B} \quad (10)$$

The effective conductivity of the pore electrolyte in the anode, as function of filling degree, is 0.03–93 S m^{-1}, Fig. 10. Since the conductivity of pure nickel metal is quite high, it might be high contact resistance caused by the low clamping pressure, that was only 1/5 of usual value around 2 kg cm^{-2}. The obtained

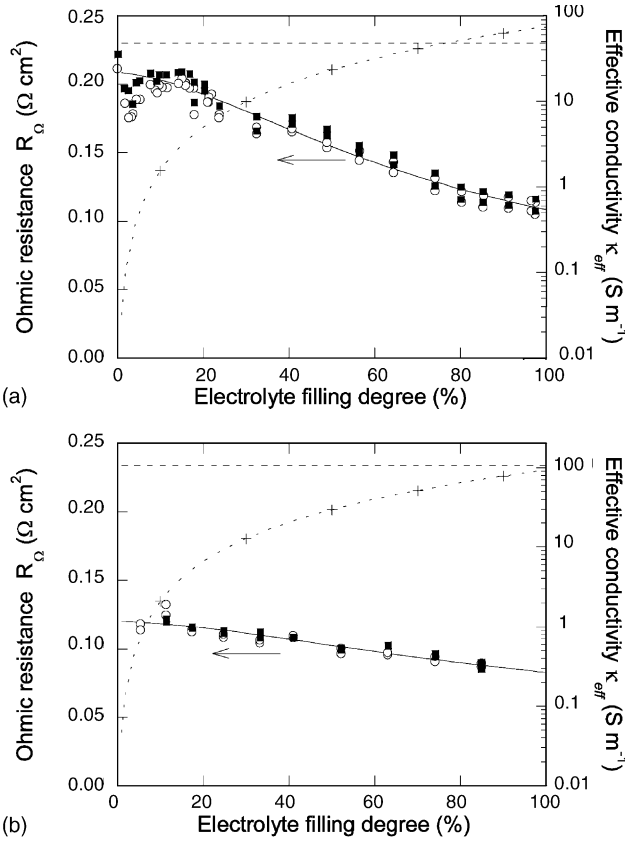

Fig. 10. The ohmic resistance at the high-frequency limit and the estimated conductivity dependence on the electrolyte filling degree for anodes (a) A and (b) B; (◯) standard gas, (●) coal gas, (—) fitted results, (+) effective conductivity of electrolyte, (- - -) conductivity of electrode.

impedance plot was still of the same order as the one obtained by Yuh and Selman [11]. However, it should also be noted that the conductivity of the pore electrolyte in the electrode dominantly affects the ohmic resistance.

Usually the resistance at a frequency smaller than 1 kHz is treated as the 'internal resistance' of the MCFC [12]. It has been construed that the 'internal resistance' is the sum of the resistance of pore electrolyte in the matrix and contact resistance between the metals. However, it becomes clear in this study that the 'internal resistance' also depends on the resistance of the pore electrolyte in the electrode.

3.5. Analysis of the reaction rate distribution in porous electrodes

In order to evaluate if the use of the equivalent circuit is valid, and if a simple model can explain the reported oxidation of the anode [1], the following model was used.

According to Newman and Tobias [13] the dimensionless reaction rate for a porous electrode, with linear polarization equation and uniform concentration, is given by:

$$\frac{\mathrm{d}j_2}{\mathrm{d}y} = \frac{\kappa_{\text{eff}}\nu}{(\sigma_{\text{eff}} + \kappa_{\text{eff}})\sinh(\nu)} \left[\cosh(\nu y) - \frac{\sigma_{\text{eff}}}{\kappa_{\text{eff}}}\cosh[(1-y)\nu]\right] \quad (11)$$

where

$$j_2 = \frac{i_2}{i}, y = \frac{x}{L_{\text{electrode}}}, \nu = L_{\text{electrode}}\sqrt{\frac{S_{\text{spec}}}{R_a}\left(\frac{1}{\sigma_{\text{eff}}} + \frac{1}{\kappa_{\text{eff}}}\right)}$$

Sparr et al. [14] found that the gas composition inside the electrode and current collector is almost uniform for low and medium electrolyte filling degrees if the gas is assumed to be in equilibrium when entering the current collector. At very high filling degrees, the gas phase mass transport will increase and finally a very small part of the electrode might only be available for reaction and would lead to a non-uniform reaction distribution.

Note that the parameter ν gives uniformity of reaction rate in the electrode. For example, for the case ($\nu \to 0$), the value of dj_2/dy becomes 1.

The dimensionless reaction rate of anode A as a function of the dimensionless electrode depth is shown in Fig. 11. The presented experimental results have been used in the calculations. At low filling degree, the conductivity in the pore electrolyte is low, and much of the electronic current enters the electrode matrix phase near the electrode/electrolyte matrix interface.

In the case of 10% electrolyte filling, the reaction rate close to the matrix is about five times higher than the average reaction rate in the electrode. Oxidation and agglomeration of the nickel particles were observed under the operation with coal gas [1]. The more uneven current distribution for coal gas than for standard gas causes a non-uniform potential distribution; this might be a contribution to the anode oxidation that was observed near the electrode/electrolyte matrix interface in the case of low filling degree. However, further work is still necessary to explain this oxidation of the anode.

In Fig. 12, the parameter υ is shown as a function of the electrolyte filling degree. The curve for the anode becomes steep below 15% filling degree for both gas compositions. This result suggests that the lower limit of the filling degree of the anode is around 15%; in order to avoid non-uniform distribution of the reaction in the electrode the filling degree should be higher. It must be kept in mind that a model including the effect of gas phase mass transfer would give a more even current distribution than this model.

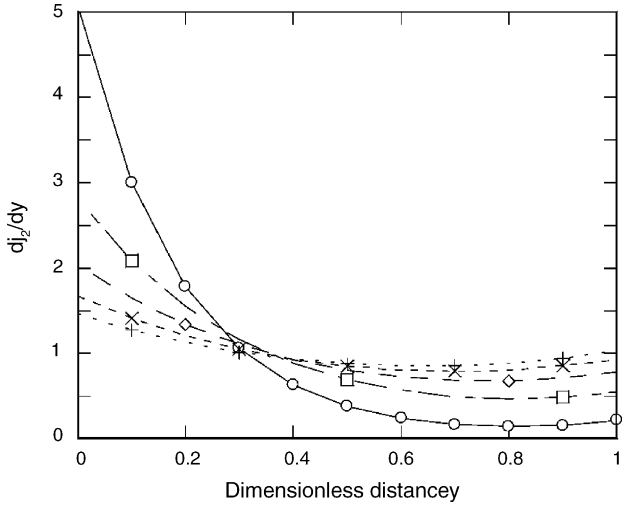

Fig. 11. Calculated reaction rate distribution in anode A for coal gas at different electrolyte filling degrees (◯) 10%, (□) 20%, (◊) 30%, (×) 40%, (+) 50%. $y = 0$ is matrix side and $y = 1$ is current collector side.

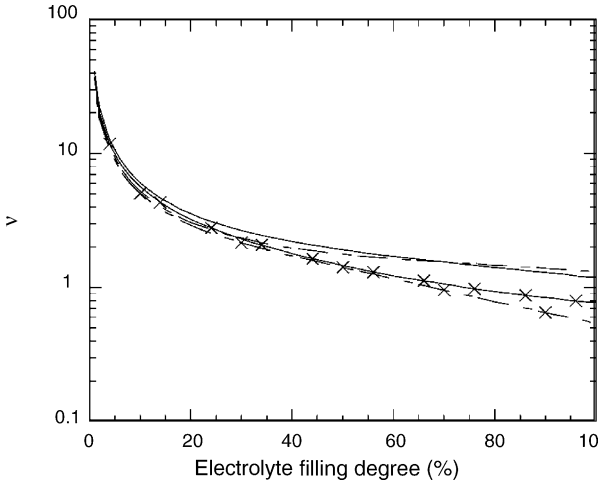

Fig. 12. The uniformity parameter, υ, dependence on electrolyte filling degree for different anodes and gas conditions, (—) standard gas, (- - -) coal gas, (no marker) anode A, (+) anode B.

This leads to the conclusion that the experimental evaluation of parameters might be very uncertain at high and low filling degrees, but will probably not be an issue in a real cell when one wants to operate at more optimal conditions. When the current distribution is uniform for a large electrolyte filling degree interval the equivalent circuit used seems valid in the electrolyte filling degree of interest.

4. Conclusions

Stationary polarization curves and electrochemical impedance spectroscopy of a porous nickel anode in a molten carbonate fuel cell were obtained in order to determine the active surface area and conductivities with varying degrees of electrolyte filling using two different gas compositions.

The impendence measurements were evaluated by a Randles–Ershler equivalent circuit. This equivalent circuit can be used to evaluate plane dense electrodes but it cannot accurately represent the actual distribution of the double layer capacitance and reaction distribution inside the electrode. But is was concluded that the current distribution is uniform for a large electrolyte filling degree interval the equivalent circuit used seems valid in the electrolyte filling degree of interest.

According to the one-dimensional model, the reaction rate on the surface is about five times higher than the average reaction rate in the electrode in the case of 10% electrolyte filling. This result suggests that the lower limit of filling of the anode is around 15%; in order to avoid non-uniform distribution of the reaction in the electrode the filling degree should be higher.

The maximum performance is obtained with a fill of about 10–50% for anode A and 5–20% for anode B in the case of operation with standard gas using Li/Na carbonate. In the case of

operation with coal gas, the optimal degree of electrolyte filling was shifted toward higher values. Regarding Li/K carbonate, no remarkable difference in optimal degree of filling between standard gas and coal gas was seen.

It was found that the active surface area for coal gas is reduced by 70–80% compared to the standard gas composition when using Li/Na carbonate. Therefore, the increase of the polarization losses when using coal gas is not only an effect of gas composition but also due to a decrease of active surface area.

An electrolyte distribution model taking into account the wetting properties of the electrode is required in order to set the optimal electrolyte filling degree of the electrode.

The effective conductivity of the anode has been determined to be 48–106 S m^{-1}, and the effective conductivity of the pore electrolyte in the anode, as a function of electrolyte filling degree, is 0.03–93 S m^{-1}. Note that the conductivity of the pore electrolyte in the electrode dominantly affects to the ohmic resistance. It means that the 'internal resistance', i.e. the resistance at a frequency lower than 1 kHz, is affected by the resistance of the pore electrolyte in the electrode.

Acknowledgements

The cell components were provided by ECN and by AIST. Mr. Tanimoto is acknowledged for the preparation of the material. The authors very much appreciate the efficient help of Dr. Carina Lagergren in solving some experimental problems and Dr. Anders Lundblad for help with Hg porosimetry measurements.

References

[1] M. Kawase, H. Morita, Y. Mugikura, Y. Izaki, CRIEPI Report W03032, 2004 (in Japanese).
[2] H. Morita, Y. Mugikura, Y. Izaki, T. Watanabe, T. Abe, Denki Kagaku (Electrochem.) 65 (1997) 740–746 (in Japanese).
[3] M. Kawase, Y. Mugikura, T. Watanabe, J. Electrochem. Soc. 147 (3) (2000) 854–860.
[4] C.Y. Yuh, Ph.D. Thesis, Illinois Institute of Technology, Chicago, Illinois, 1985.
[5] J.R. McDonald, Impedance Spectroscopy, John Wiley & Sons, Inc., New York, 1987.
[6] J.A. Prins-Jansen, G.A.J.M. Plevier, K. Hemmes, J.H.W. de Wit, Electrochim. Acta 41 (1996) 1323–1329.
[7] J.R. Selman, Y.P. Lin, Electrochim. Acta 38 (1993) 2063–2073.
[8] T. Nishina, M. Takahashi, I. Uchida, J. Electrochem. Soc. 137 (1990) 1112–1121.
[9] R. Weewer, R.C. Makkus, K. Hemmes, J.H. de Wit, J. Electrochem. Soc. 137 (1990) 3156–3157.
[10] R. Hilfer, Adv. Chem. Phys. 92 (1996) 299–424.
[11] C.Y. Yuh, J.R. Selman, AlChE J. 34 (1988) 1949–1958.
[12] Y. Mugikura, K. Shimazu, T. Watanabe, Y. Izaki, T. Abe, H. Urushibata, H. Maeda, K. Sato, T. Murahashi, Denki Kagaku (Electrochem.) 60 (1992) 117–123 (in Japanese).
[13] J. Newman, C. Tobias, J. Electrochem. Soc. 109 (12) (1962) 1183–1191.
[14] M. Sparr, A. Bodén, G. Lindbergh, J. Electrochem. Soc., submitted for publication.